LETTER

doi:10.1038/nature19815

Allogeneic transplantation of iPS cell–derived cardiomyocytes regenerates primate hearts

Yuji Shiba[1,2]*, Toshihito Gomibuchi[3]*, Tatsuichiro Seto[3], Yuko Wada[3], Hajime Ichimura[3], Yuki Tanaka[3], Tatsuki Ogasawara[3], Kenji Okada[3], Naoko Shiba[4], Kengo Sakamoto[5], Daisuke Ido[5], Takashi Shiina[6], Masamichi Ohkura[7,8], Junichi Nakai[7,8], Narumi Uno[9], Yasuhiro Kazuki[9], Mitsuo Oshimura[9], Itsunari Minami[10] & Uichi Ikeda[2]

Induced pluripotent stem cells (iPSCs) constitute a potential source of autologous patient-specific cardiomyocytes for cardiac repair, providing a major benefit over other sources of cells in terms of immune rejection. However, autologous transplantation has substantial challenges related to manufacturing and regulation. Although major histocompatibility complex (MHC)-matched allogeneic transplantation is a promising alternative strategy[1], few immunological studies have been carried out with iPSCs. Here we describe an allogeneic transplantation model established using the cynomolgus monkey (*Macaca fascicularis*), the MHC structure of which is identical to that of humans. Fibroblast-derived iPSCs were generated from a MHC haplotype (HT4) homozygous animal and subsequently differentiated into cardiomyocytes (iPSC-CMs). Five HT4 heterozygous monkeys were subjected to myocardial infarction followed by direct intra-myocardial injection of iPSC-CMs. The grafted cardiomyocytes survived for 12 weeks with no evidence of immune rejection in monkeys treated with clinically relevant doses of methylprednisolone and tacrolimus, and showed electrical coupling with host cardiomyocytes as assessed by use of the fluorescent calcium indicator G-CaMP7.09. Additionally, transplantation of the iPSC-CMs improved cardiac contractile function at 4 and 12 weeks after transplantation; however, the incidence of ventricular tachycardia was transiently, but significantly, increased when compared to vehicle-treated controls. Collectively, our data demonstrate that allogeneic iPSC-CM transplantation is sufficient to regenerate the infarcted non-human primate heart; however, further research to control post-transplant arrhythmias is necessary.

Human iPSCs, like human embryonic stem (ES) cells, are a promising cell source for cardiac repair because of their unlimited self-renewal and ability to differentiate into cardiomyocytes[2–4]. Theoretically, human iPSCs could be used for autologous transplantation; however, it is not clear whether this strategy will be feasible in a clinical setting because it is time-consuming, laborious, and costly. This is particularly true for heart regeneration, which requires a large number of cells[2]. Allogeneic transplantation of iPSC-CMs could solve these practical issues. A potential disadvantage of allogeneic transplantation is that it can induce an immune response, which might cause graft rejection. The MHC plays an essential role in the post-transplant immune response[5] and graft-versus-host disease[6]; therefore, the use of MHC-matched transplants is a potential approach to avoid rejection. In the present study, we investigated whether MHC-matched allogeneic iPSC-CMs can survive in the long term following transplantation without forming tumours in a non-human primate myocardial infarction model. Additionally, we assessed the mechanical and electrical consequences of transplantation in this clinically relevant model.

We screened the MHC RNA sequences of Filipino cynomolgus monkeys and identified an animal with strictly homozygous MHC-class I (ref. 7) and MHC-class II (ref. 8) regions on both chromosomes (named HT4, Extended Data Fig. 1a, b). We designated this HT4 homozygous animal as an iPSC donor and isolated skin fibroblasts from the animal. iPSCs were established by transfection with plasmid vectors encoding *OCT4* (also known as *POU5F1*), *SOX2*, *KLF4* and *L-MYC* (*MYCL*) and subsequently formed typical ES-cell-like colonies (Extended Data Fig. 2a), expressed pluripotent markers (Extended Data Fig. 2b–f) and displayed the ability to form teratomas (Extended Data Fig. 2g–i). We previously used a human ES cell line expressing the fluorescent calcium indicator GCaMP3 to show that grafted cardiomyocytes could couple with host cardiomyocytes in an injured guinea-pig heart[9,10]; however, we were unable to detect sufficient fluorescent signals from GCaMP3-expressing iPSC-CMs in a monkey heart in our system (data not shown), suggesting a need for an indicator with enhanced fluorescence. As such, we developed a fluorescent calcium indicator, G-CaMP7.09 (Extended Data Fig. 3a), which was transfected into undifferentiated cynomolgus monkey iPSCs. After expansion, the majority of G-CaMP7.09-expressing cells showed fluorescence, and 14 out of 15 metaphases displayed a normal karyotype (42, XY; Extended Data Fig. 2j). Next, we generated iPSC-CMs using our previously reported protocol[9,11] as modified by another group[12]. Because incubation of iPSC derivatives in glucose-free medium[13] for 3 days significantly increased the fraction of cardiomyocytes ($P < 0.01$) in a preliminary experiment (Extended Data Fig. 4a), we added this selection step following cardiac differentiation in the present study (Extended Data Fig. 5a). We prepared 4×10^8 cardiomyocytes for a recipient animal (cardiac troponin T (cTnT)-positive, $83.8 \pm 1.0\%$; Extended Data Fig. 4b–f), and the cells were heat-shocked[14] before cryopreservation. Consistent with our previous work[15], the expression of cTnT was lower in iPSC-CMs than in adult hearts (Extended Data Fig. 4g), indicative of cellular immaturity. Cells were treated with our previously reported pro-survival cocktail (PSC) before transplantation[11,16], and post-thawing viability as indicated by trypan blue staining was $74.5 \pm 4.1\%$. Spontaneous beating was observed *in vitro*, which was synchronous with the fluorescent transients of G-CaMP7.09 (Extended Data Fig. 3b–e, Supplementary Video 1). Consistent with previous work[17], the firing rate of G-CaMP7.09 fluorescence was substantially decreased after ryanodine treatment (Extended Data Fig. 3c). Treatment with the l-type calcium-channel blocker nifedipine led to cessation of firing (Extended Data Fig. 3d), whereas the addition of caffeine—which opens sarcoplasmic reticulum ryanodine channels—promoted firing fluorescence (Extended Data Fig. 3e). Note that firing fluorescence always corresponded with contraction under all conditions (Supplementary Video 2). To exclude

[1]Institute for Biomedical Sciences, Shinshu University, Matsumoto 390-8621, Japan. [2]Department of Cardiovascular Medicine, Shinshu University School of Medicine, Matsumoto 390-8621, Japan. [3]Department of Cardiovascular Surgery, Shinshu University School of Medicine, Matsumoto 390-8621, Japan. [4]Department of Pediatrics, Shinshu University School of Medicine, Matsumoto 390-8621, Japan. [5]Ina Research Inc., Ina 399-4501, Japan. [6]Department of Molecular Life Science, Tokai University School of Medicine, Isehara 259-1193, Japan. [7]Brain Science Institute, Saitama University, Saitama 338-8570, Japan. [8]Graduate School of Science and Engineering, Saitama University, Saitama 338-8570, Japan. [9]Chromosome Engineering Research Center, Tottori University, Yonago 683-8503, Japan. [10]Institute for Integrated Cell-Material Sciences (WPI-iCeMS), Kyoto University, Kyoto 606-8501, Japan.
*These authors contributed equally to this work.

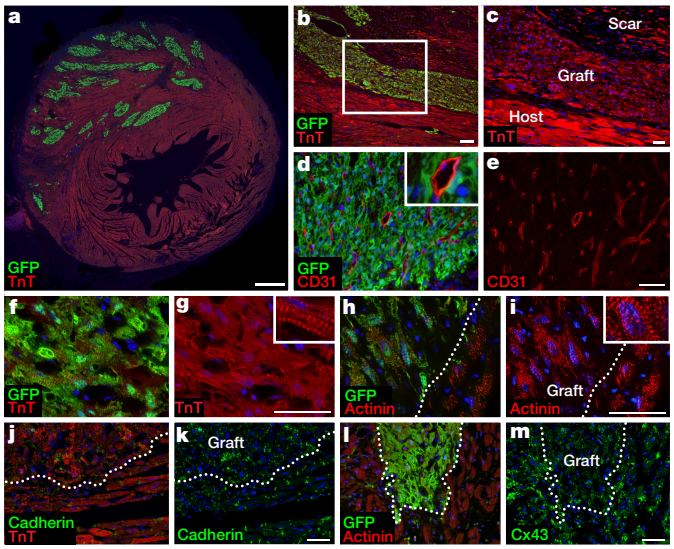

Figure 1 | Transplanted iPSC-CMs partially remuscularize infarcted cynomolgus monkey hearts. a–m, Fluorescence microscopic images of cynomolgus monkey hearts subjected to myocardial infarction and transplantation of iPSC-CMs. Grafts were studied on day 84 post-transplantation. **a**, A substantial number of grafted cardiomyocytes (green) survived in the anterior portion of the left ventricle. Scale bar, 1 mm. **b**, **c**, Grafted cells located in the border zone. Note that almost all of the GFP$^+$ cells are cTnT$^+$. **c**, Enlargment of the box in **b**. Scale bars, 100 μm (**b**) and 50 μm (**c**). **d**, **e**, Graft cardiomyocytes were well vascularized by the host-derived (GFP$^-$/CD31$^+$) endothelial cells. Representative endothelium is shown with higher magnification in the inset in **d**. Scale bar, 50 μm. **f–i**, Graft cardiomyocytes showed sarcomeric structures identified by cTnT and α-actinin (Actinin) staining. Representative sarcomeric structures with higher magnification are shown in the insets in **g**, **i**. Scale bars, 50 μm. **j–m**, Expression of cell adhesion protein pan-cadherin (Cadherin) and gap junction protein connexin 43 (Cx43) in the graft and host tissue. Scale bars, 50 μm. **f**, **g**; **h**, **i**; **j**, **k**; and **l**, **m** denote paired images. **h–m**, Dashed lines indicate the border between graft and host tissues.

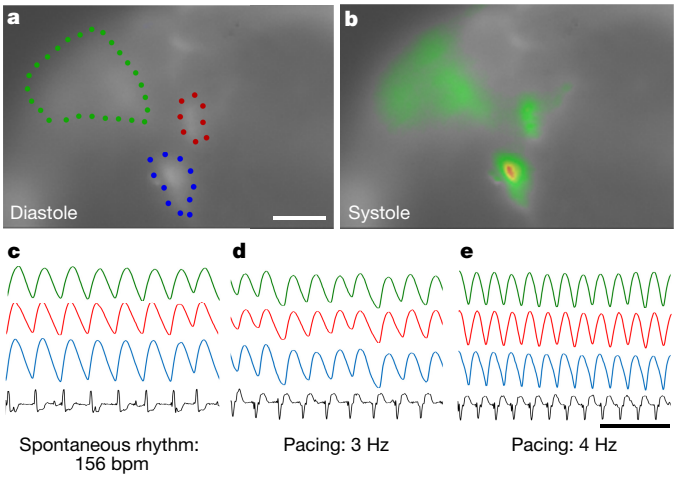

Figure 2 | iPSC-CMs electrically couple with the host heart. **a**, **b**, Intravital fluorescence image of the Langendorff-perfused heart showing flashing (dotted lines) fluorescence of the calcium indicator, G-CaMP7.09, in the heart. Scale bar, 2 mm. **c–e**, G-CaMP7.09 fluorescent signals for green, red, and blue regions of interest indicated in **a**, as well as the ECG (black). Contractions in all three regions are synchronous with the host ECG when the heart beats spontaneously and is paced at ≤4 Hz (240 bpm). Scale bar, 1 s.

the possibility that the G-CaMP7.09 transients were generated by stretch-activated calcium intake, we cultured G-CaMP7.09-expressing iPSC-CMs on stretchable Parafilm. When the cells were treated with 40 mM 2,3-butanedione 2-monoxime (BDM), the cardiomyocytes stopped beating, whereas G-CaMP7.09 transients were sustained for a few minutes (Extended Data Fig. 3f, Supplementary Video 3). After cessation of the fluorescent transients, no G-CaMP7.09 signal was observed in response to passive stretching, but treatment with caffeine restored the G-CaMP7.09 transients (Extended Data Fig. 3g, h). These findings strongly indicate that the G-CaMP7.09 fluorescent transients in iPSC-CMs are reflective of their contraction via calcium-induced calcium release from ryanodine receptors.

We first transplanted 4×10^8 iPSC-CMs suspended in PSC into MHC-mismatched monkeys treated with methylprednisolone and tacrolimus ($n = 2$) and found that grafted cardiomyocytes were thoroughly rejected as the result of severe infiltration of T lymphocytes 4 weeks after transplantation, as determined by histological analysis (Extended Data Fig. 6a, b). Subsequently, ten 4–5-year-old female cynomolgus monkeys were used as recipient animals. Five monkeys in which either of the MHC haplotypes was identical to that of the donor (HT4, Extended Data Fig. 1a) received iPSC-CMs and the other received PSC vehicle (Extended Data Fig. 5b); all animals were treated with methylprednisolone and tacrolimus. *In vitro* mixed lymphoid reactions indicated no or little immune response when HT4 homozygous cells were cocultured with HT4 heterozygous cells (Extended Data Fig. 1c). Myocardial infarction was induced by 3 h ischaemia followed by reperfusion (Supplementary Video 4). Two weeks later, either 4×10^8 iPSC-CMs suspended in PSC or vehicle alone were injected into the infarct zone and the border zone. Animals were euthanized and underwent full necropsy 12 weeks post-transplantation. None showed any macro- or microscopic tumour formation (Extended Data Fig. 7a–h). All animals showed patchy scar formation in the heart (percentage scar area/left ventricle area: 10.2 ± 0.7% (PSC vehicle) and 8.8 ± 1.0% (iPSC-CMs), $P = 0.30$, Extended Data Fig. 8a). The average plasma tacrolimus trough level 12 weeks post-transplantation was 24.4 ± 3.1 ng ml^{-1} and 22.2 ± 2.2 ng ml^{-1} in PSC-vehicle and iPSC-CM recipient animals, respectively. The iPSC-CM recipients showed partial remuscularisation of the scar tissue by the grafted cardiomyocytes (percentage graft area/scar area: 16.3 ± 5.0%, Fig. 1a–c and Extended Data Fig. 7i–p), which was well vascularised by the host vessels (Fig. 1d, e). More than 99% of the graft GFP$^+$ cells were cTnT$^+$ cardiomyocytes (Fig. 1b, c). Despite the lower overall expression of cTnT in iPSC-CMs in the graft compared to host CMs (Fig. 1c and Extended Data Fig. 4g), grafted cardiomyocytes showed clear sarcomere structure with cTnT and α-actinin (Fig. 1f–i). Grafts localized to the border zone and within the scar area (Extended Data Fig. 7i–p). Additionally, some grafts were surrounded by scar tissue and appeared to be isolated from the host myocardium (Fig. 1b, c). However when we looked at the same grafts at different levels of section, we could see that most were in direct contact with host cardiomyocytes (Extended Data Fig. 7l–n). Expression of the cell adhesion protein cadherin and the gap junction protein connexin 43 was observed in the grafts, but was relatively rare compared to that in the host (Fig. 1j–m). Immunohistochemical staining for CD45 (leukocytes), CD3 (T lymphocytes), and CD20 (B lymphocytes) on day 84 post-transplantation revealed no evidence of acute graft rejection (Extended Data Fig. 6c–i).

To confirm electrical coupling of the grafted cardiomyocytes to the host heart, all iPSC-CM-transplanted hearts were subjected to intravital G-CaMP7.09 fluorescence imaging. After deep anaesthesia, the heart was perfused with cold cardioplegia solution, excised, and transported to a Langendorff setup. Next, it was reperfused with oxygenated Tyrode's solution and resumed spontaneous beating, and G-CaMP signalling and electrocardiograms (ECGs) were recorded. We observed multiple flashing fluorescent signals that were synchronous with each other and with the host ECG in all five animals (Fig. 2a–e, Supplementary Video 5, and Extended Data Fig. 8a). Grafted cardiomyocytes showed 1:1 coupling with host cardiomyocytes (Fig. 2c–e), but graft activation was delayed when the hearts were paced at 4 Hz

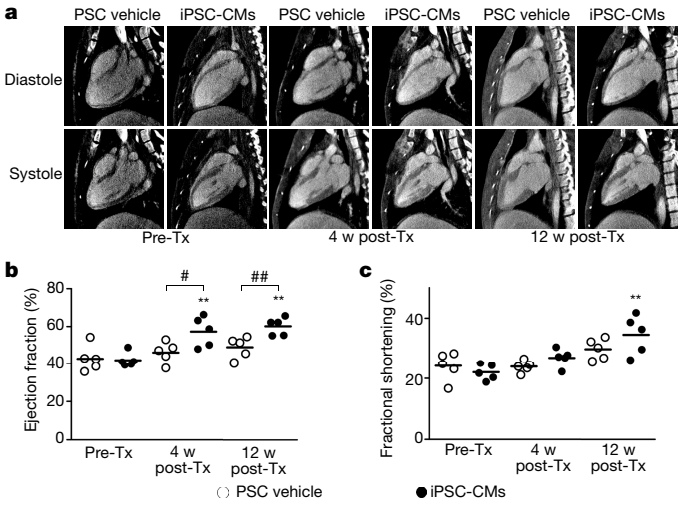

Figure 3 | Transplantation of iPSC-CMs improves cardiac contractile function. Cardiac contractile function was evaluated before transplantation (Pre-Tx) and at 4 weeks post-transplantation (4 w post-Tx) and 12 weeks post-transplantation (12 w post-Tx) by μCT and echocardiography. **a**, Representative longitudinal axis diastolic and systolic μCT images. **b**, Ejection fraction as assessed by μCT. **c**, Fractional shortening as assessed by echocardiography. $n = 5$ in each group. $^{\#}P < 0.05$, $^{\#\#}P < 0.01$ between vehicle and iPS-CM; $^{**}P < 0.01$ versus Pre-Tx.

(Extended Data Fig. 9a, b). This slower propagation probably reflects the limited formation of gap junctions in the graft tissue (Fig. 1m). To evaluate cardiac contraction, we used a novel micro-computed tomography (μCT) system (Fig. 3a), as well as echocardiography. Contractile function analysis by μCT in intact cynomolgus monkeys ($n = 5$) revealed consistent ejection fractions ($64.6 \pm 1.5\%$). Echocardiography and μCT were performed on days −2, 28 and 84 relative to transplantation (Fig. 3a–c and Extended Data Fig. 10a–d). Echocardiography-based analysis of fractional shortening revealed that shortening in iPSC-CM recipients tended to be higher, albeit not significantly, than in vehicle-treated recipients on days 28 and 84. Fractional shortening in transplanted animals improved significantly only on day 84 compared to day −2 (Fig. 3c). μCT analysis seemed to be superior to echocardiography for evaluating apical cardiac contraction (Supplementary Video 6) because contractile function of the apex was generally difficult to evaluate by echocardiography after sternotomy, owing to post-operative adhesion. Furthermore, the ejection fraction was significantly higher in the iPSC-CM recipients than in vehicle-treated animals on days 28 and 84 and compared to pre-transplantation readings as analysed by μCT (Fig. 3b). There was also a reasonable negative correlation between scar size and ejection fraction ($r = -0.67$, Extended Data Fig. 8b) and a positive correlation between graft size and ejection fraction ($r = 0.91$, Extended Data Fig. 8c). In vehicle-treated animals, the plasma B-type natriuretic peptide (BNP) level was highest on day 0 and gradually declined throughout the experimental period (the BNP levels on days 56 and 84 were significantly lower than on day 0); although the levels in iPSC-CM recipients tended to increase on day 28 when compared to day 0, they decreased on days 56 and 84. However, BNP levels did not differ significantly between the two groups at any time point (Extended Data Fig. 10e).

To assess the electrophysiological consequences of iPSC-CM grafting, the animals were subjected to Holter ECG monitoring on days −2, 7, 14, 28, 42, 56, 70 and 80 relative to the day of transplantation. No ventricular tachycardia was observed before transplantation in either iPSC-CM or vehicle recipients. Episodes of sustained ventricular tachycardia (Fig. 4a) were observed only after transplantation. The duration of the sustained ventricular tachycardia peaked at day 14 and shortened considerably thereafter in 4 out of 5 animals (Fig. 4b and Extended Data Fig. 8d). Similarly, the incidence of any (sustained or non-sustained) ventricular tachycardia (Fig. 4c and Extended Data Fig. 9c–f) and sustained ventricular tachycardia (Fig. 4d) peaked on day 14 and declined gradually throughout the rest of the study period. Notably, while all of the recipients of iPSC-CMs showed sustained ventricular tachycardia on day 14, none was apparent on days 56 and 84 (Fig. 4d). The fastest observed ventricular tachycardia exceeded 240 bpm (beats per minute) (Extended Data Fig. 8d), but none of the animals showed any abnormal behaviour, such as syncope, throughout the study period.

This study demonstrated that allogeneic transplantation of MHC-matched iPSC-CMs can provide long-term graft survival in the infarcted hearts of non-human primates. Both MHC and minor antigens[18–20] have been shown to play important roles in the immune response following allogeneic transplantation. In fact, one research group recently observed graft rejection following MHC-matched iPSC-CM transplantation into the subcutaneous tissue of allogeneic cynomolgus monkeys[21]. Given that grafted cardiomyocytes survived for 12 weeks without immune rejection in all five iPSC-CM recipients in this study, it is reasonable to assume that a combination of methylprednisolone and tacrolimus is sufficient to prevent immune rejection of transplanted allogeneic cardiomyocytes. Nevertheless, further studies are required to establish the minimum amount of immunosuppression required to control immune rejection following cell transplantation.

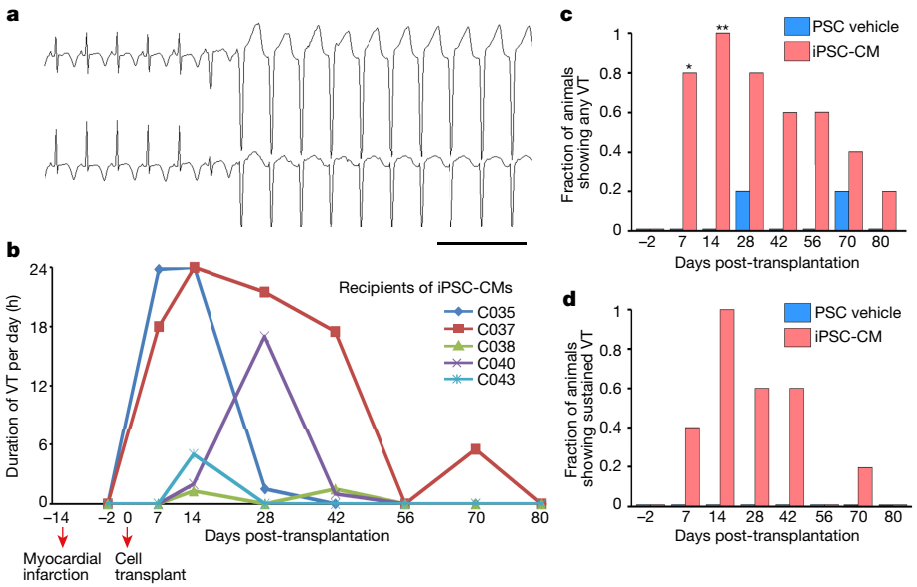

Figure 4 | Electrical consequences of transplantation of iPSC-CMs. **a**, Representative traces of ventricular tachycardia (VT) in a recipient of iPSC-CMs. Scale bar, 1 s. **b**, Duration of sustained ventricular tachycardia in iPSC-CM recipients. Note that none of the recipients of PSC vehicle showed sustained ventricular tachycardia throughout the study period. **c**, Fraction of animals showing any (sustained or non-sustained) ventricular tachycardia. **d**, Fraction of animals showing sustained ventricular tachycardia. $n = 5$ in each group. $^{*}P < 0.05$; $^{**}P < 0.01$ versus PSC vehicle.

We also demonstrated that iPSC-CMs integrated and improved cardiac contractile function in a primate infarct model. Demonstration of electrically coupled grafts strongly supports the notion that grafted cardiomyocytes improve cardiac contractile function by creating new force-generating units, although other mechanisms—such as paracrine effects—cannot be excluded.

Although our previous study showed that transplantation of human cardiomyocytes suppressed ventricular arrhythmias in injured guinea-pig hearts[9], Chong *et al.* observed post-transplant arrhythmias in the non-human primate heart after human ES-cell-derived cardiomyocyte transplantation[22]. The most likely reason for these inconsistencies is that the non-human primate heart is more similar to the human heart than the hearts of rodents with respect to size and beating rate. It is noteworthy that allogeneic transplantation in large animal models, as is the case in clinical studies, is thought to be the most sensitive model to detect post-transplant arrhythmias. In fact, although idioventricular rhythms represented the majority of sustained ventricular arrhythmias observed in the xenogeneic transplantation study[22], our study demonstrated that allogeneic transplantation of iPSC-CMs significantly increased the incidence of ventricular tachycardia. The incidence of sustained ventricular tachycardia did not seem to correlate with graft size, coupled graft number, scar size or cardiac contractile function in our study (Extended Data Fig. 8a, d). The reduced incidence of ventricular tachycardia over time may reflect the reduced portion of grafted cardiomyocytes; however, pluripotent stem cell-derived cardiomyocytes have been shown to proliferate *in vivo* and the graft area grew until 4 weeks post-transplantation[14]. A more likely possibility is that the decreased incidence of ventricular tachycardia resulted from maturation of graft CMs *in vivo*[22]. Notably, all iPSC-CM recipients survived for 12 weeks until the end of the study without any abnormal behaviour, and post-transplant arrhythmias seemed to be transient, peaking on day 14 post-transplantation and gradually decreasing thereafter. These results suggest that iPSC-CM transplant-induced ventricular tachycardia was non-lethal and transient.

There are a few limitations in the study design. First, we tested only one iPS cell line, so additional studies using multiple cell lines will be required. Second, our animal model is not always clinically relevant in view of its relatively small infarct size in young adolescent monkeys. Finally, the 12-week observation period after cell transplantation does not allow a definitive conclusion regarding graft survival without chronic rejection and a longer follow-up study will be required to investigate chronic rejection and the risks associated with immunosuppressant use further.

In conclusion, allogeneic transplantation of iPSC-CMs led to integrated graft survival and improved cardiac contractility for at least 12 weeks in a non-human primate myocardial infarction model. Transient, non-lethal ventricular tachycardia was significantly increased by the iPSC-CMs, generating the need for more effort to control arrhythmias before clinical application.

Online Content Methods, along with any additional Extended Data display items and Source Data, are available in the online version of the paper; references unique to these sections appear only in the online paper.

Received 7 October 2015; accepted 31 August 2016.
Published online 10 October 2016.

1. Deleidi, M., Hargus, G., Hallett, P., Osborn, T. & Isacson, O. Development of histocompatible primate-induced pluripotent stem cells for neural transplantation. *Stem Cells* **29,** 1052–1063 (2011).
2. Laflamme, M. A. & Murry, C. E. Heart regeneration. *Nature* **473,** 326–335 (2011).
3. Lalit, P. A., Hei, D. J., Raval, A. N. & Kamp, T. J. Induced pluripotent stem cells for post-myocardial infarction repair: remarkable opportunities and challenges. *Circ. Res.* **114,** 1328–1345 (2014).
4. Shiba, Y., Hauch, K. D. & Laflamme, M. A. Cardiac applications for human pluripotent stem cells. *Curr. Pharm. Des.* **15,** 2791–2806 (2009).
5. Bach, F. H., Bach, M. L. & Sondel, P. M. Differential function of major histocompatibility complex antigens in T-lymphocyte activation. *Nature* **259,** 273–281 (1976).
6. Petersdorf, E. W. The major histocompatibility complex: a model for understanding graft-versus-host disease. *Blood* **122,** 1863–1872 (2013).
7. Shiina, T. *et al.* Discovery of novel MHC-class I alleles and haplotypes in Filipino cynomolgus macaques (*Macaca fascicularis*) by pyrosequencing and Sanger sequencing: Mafa-class I polymorphism. *Immunogenetics* **67,** 563–578 (2015).
8. Blancher, A. *et al.* Study of MHC class II region polymorphism in the Filipino cynomolgus macaque population. *Immunogenetics* **66,** 219–230 (2014).
9. Shiba, Y. *et al.* Human ES-cell-derived cardiomyocytes electrically couple and suppress arrhythmias in injured hearts. *Nature* **489,** 322–325 (2012).
10. Shiba, Y. *et al.* Electrical integration of human embryonic stem cell-derived cardiomyocytes in a guinea pig chronic infarct model. *J. Cardiovasc. Pharmacol. Ther.* **19,** 368–381 (2014).
11. Laflamme, M. A. *et al.* Cardiomyocytes derived from human embryonic stem cells in pro-survival factors enhance function of infarcted rat hearts. *Nat. Biotechnol.* **25,** 1015–1024 (2007).
12. Zhang, J. *et al.* Extracellular matrix promotes highly efficient cardiac differentiation of human pluripotent stem cells: the matrix sandwich method. *Circ. Res.* **111,** 1125–1136 (2012).
13. Tohyama, S. *et al.* Distinct metabolic flow enables large-scale purification of mouse and human pluripotent stem cell-derived cardiomyocytes. *Cell Stem Cell* **12,** 127–137 (2013).
14. Laflamme, M. A. *et al.* Formation of human myocardium in the rat heart from human embryonic stem cells. *Am. J. Pathol.* **167,** 663–671 (2005).
15. Minami, I. *et al.* A small molecule that promotes cardiac differentiation of human pluripotent stem cells under defined, cytokine- and xeno-free conditions. *Cell Reports* **2,** 1448–1460 (2012).
16. Gautam, M. *et al.* Transplantation of adipose tissue-derived stem cells improves cardiac contractile function and electrical stability in a rat myocardial infarction model. *J. Mol. Cell. Cardiol.* **81,** 139–149 (2015).
17. Li, J., Qu, J. & Nathan, R. D. Ionic basis of ryanodine's negative chronotropic effect on pacemaker cells isolated from the sinoatrial node. *Am. J. Physiol.* **273,** H2481–H2489 (1997).
18. Derks, R. A., Jankowska-Gan, E., Xu, Q. & Burlingham, W. J. Dendritic cell type determines the mechanism of bystander suppression by adaptive T regulatory cells specific for the minor antigen HA-1. *J. Immunol.* **179,** 3443–3451 (2007).
19. Kwun, J. *et al.* Impact of leukocyte function-associated antigen-1 blockade on endogenous allospecific T cells to multiple minor histocompatibility antigen mismatched cardiac allograft. *Transplantation* **99,** 2485–2493 (2015).
20. Vokaer, B. *et al.* Critical role of regulatory T cells in Th17-mediated minor antigen-disparate rejection. *J. Immunol.* **185,** 3417–3425 (2010).
21. Kawamura, T. *et al.* Cardiomyocytes derived from MHC-homozygous induced pluripotent stem cells exhibit reduced allogeneic immunogenicity in MHC-matched non-human primates. *Stem Cell Reports* **6,** 312–320 (2016).
22. Chong, J. J. *et al.* Human embryonic-stem-cell-derived cardiomyocytes regenerate non-human primate hearts. *Nature* **510,** 273–277 (2014).

Supplementary Information is available in the online version of the paper.

Acknowledgements We thank Y. Ichihara, N. Ishimine, Y. Karatsu, the Rigaku Corporation, Brainvision Inc. and the Keyence Corporation for assistance with the experiments and Astellas Pharma Inc. for the gift of tacrolimus. We also appreciate the scientific advice of M. A. Laflamme, J. Chong and N. Saito. This work was supported by research grants (to Y.S.) from the Japan Society for the Promotion of Science KAKENHI (grant no. 26293182), Japan Agency for Medical Research and Development, Takeda Science Foundation, Astellas Foundation for Research on Metabolic Disorders, Mochida Memorial Foundation for Medical and Pharmaceutical Research, and Japan Heart Association. The experiments to generate the G-CaMP7.09 plasmid were supported by grants from the Ministry of Education, Culture, Sports, Science and Technology (MEXT) to J.N. (grant no. 26115504) and M.O. (grant no. 25116504) and a grant from the Regional Innovation Cluster Program (City Area Type, Central Saitama Area) to J.N.

Author Contributions Y.S. designed the study. Y.S., T.G., T.Se., Y.W., H.I., Y.T., K.S. and D.I. performed all animal procedures. T.O., N.S. and Y.S. performed histological analysis. K.S. and D.I. analysed Holter ECGs. N.U., Y.K., and M.Os. performed karyotype analysis of iPSCs. T.Sh. analysed RNA sequences of cynomolgus MHC. K.O. and U.I. analysed all other data and provided administrative assistance. M.Oh. and J.N. generated the G-CaMP7.09 plasmid. *In vitro* fluorescent imaging studies were performed by I.M. The manuscript was written by Y.S., T.Sh., M.Oh., I.M. and N.U.

Author Information Reprints and permissions information is available at www.nature.com/reprints. The authors declare competing financial interests: details are available in the online version of the paper. Readers are welcome to comment on the online version of the paper. Correspondence and requests for materials should be addressed to Y.S. (yshiba@shinshu-u.ac.jp).

Reviewer Information *Nature* thanks T. Braun, K. Fukuda, T. Kamp and the other anonymous reviewer(s) for their contribution to the peer review of this work.

METHODS

Screening for cynomolgus monkeys with MHC homologous and heterozygous haplotypes. Total RNA was isolated from peripheral white blood cells using TRIzol reagent (Thermo Fisher Scientific) and treated with DNase I (Thermo Fisher Scientific). cDNA was synthesized using ReverTra Ace (Toyobo) with oligo d(T) primer. A set of previously reported cynomolgus macaque MHC (*Mafa*) class I-specific primers was used for RT–PCR amplification[7], and *Mafa-DRB*, *Mafa-DQA1, Mafa-DQB1, Mafa-DPA1*, and *Mafa-DPB1* were amplified with the following specific primers: *Mafa-DRB* (DRB_PHI_F1, 5′-GCTCCCTGGAGGCTCCTG-3′; DRB_PHI_R1-1, 5′-ACCAGGAGGGTGTGGTGC-3′; DRB_PHI_R1-2, 5′-ACCAGCAGGGTGTGGTGC-3′; DRB_PHI_R1-3, 5′-ACCAGGAGG TTGTGGTGC-3′ and DRB_PHI_R1-4, 5′-ACCAGGAGGCTGTGGTGC-3′), *Mafa-DQA1* (DQA_PHI_F1, 5′-ATCCTAAACAAAGCTCTG-3′ and DQA_ PHI_R2, 5′-TGTGATGTTCACCACAGG-3′), *Mafa-DQB1* (DQB_PHI_F1, 5′-CTGTGACCTTGATGCTGG-3′ and DQB_PHI_R1, 5′-AGACCAGCAG GTTGTGGT-3′), *Mafa-DPA1* (DPA_PHI_F1_1, 5-ATGTTCCAGACCAG AGCT-3′; 5′-ATGTTCGAGACCAGAGCT-3′ and DPA_PHI_R1, 5′-TTGTCAATG TGGCAGATG-3′) and *Mafa-DPB1* (DPB_PHI_F2, 5′-GCCACTCCAGAGAAT TAC-3′ and DPB_PHI_R2, 5′-GAGCAGGTTGTGGTGCTG-3′).

In addition, we designed MHC-specific fusion primers containing the Roche 454 titanium adaptor (A in forward and B in reverse primer) and a 10-bp multiple identifier (MID). In brief, each 20-μl RT–PCR mixture contained 10 ng cDNA, 0.4 U high-fidelity KOD FX polymerase (Toyobo), 2× PCR buffer, each dNTP at 2 mM, and each primer at 0.5 μM. The thermal cycling program was as follows: 25 cycles at 98 °C for 10 s, 58 °C for 30 s, and 68 °C for 30 s. The PCR products were purified with the QIAquick PCR purification kit (Qiagen) and quantified by the picogreen assay (Invitrogen) in a fluoroskan ascent microplate fluorometer (Thermo Fisher Scientific). The PCR products were mixed at equimolar concentrations and then diluted according to the manufacturer's recommendations (Roche). Emulsion PCR, breaking and bead enrichment and deposition into a picotiterplate were performed according to the manufacturer's protocol (Roche). Image processing, signal correction and base calling were performed using the GS run processor version 3.0 (Roche) with full processing for shotgun or paired-end filter analysis. Quality-filtered sequence reads that passed the assembler software (single sff file) were binned into separate sequence sff files on the basis of the MID labels, using the sff file software (Roche). These files were further trimmed to remove poor-quality sequence at the end of the reads with quality values <20. The *Mafa* class I and class II alleles were assigned by matching the sequence reads with all known *Mafa* class I allele sequences in the IMGT/MHC-NHP database[23] with GS reference mapper version 3.0, using the following parameter settings: 99% and 100% matching (for class I and class II alleles, respectively), minimum overlap length of 200 and alignment identity score of 10. We selected HT4 homozygous and heterozygous animals that had the following *Mafa* class I and class II alleles: *Mafa-A1*089:03*, *Mafa-A2*05:50*, *Mafa-A3*13:03:01*, *Mafa-B*046:01:02*, *Mafa-B*050:08*, *Mafa-B*057:04*, *Mafa-B*060:02*, *Mafa-B*072:01, Mafa-B*104:03*, *Mafa-B*114:02*, *Mafa-B*144:03N*, *Mafa-I*01:12:01*, *Mafa-DRB1*03:21*, *Mafa-DRB1*10:07*, *Mafa-DQA1*01:07:01*, *Mafa-DQB1*06:08*, *Mafa-DPA1*02:05*, and *Mafa-DPB1*15:04* (Extended Data Fig. 1a). Since only 0.84% of animals showed the HT4 haplotype in either MHC, we designated HT4 heterozygous monkeys as recipients of iPSC-CMs and non-HT4 monkeys as recipients of PSC vehicle (no randomization between groups). All experiments and analyses were performed under blinded conditions. No statistical methods were used to predetermine sample size.

Generation of a G-CaMP7.09-reporter cynomolgus iPSC line. Skin fibroblasts were isolated from a male MHC-homozygous cynomolgus monkey. The fibroblasts were transfected with a combination of plasmid vectors encoding *OCT4*, *SOX2*, *KLF4*, and *L-MYC* as described previously[24]. The cynomolgus iPSCs were maintained on SNL feeder cells (Cell Biolabs) treated with mitomycin C (Sigma-Aldrich) in essential 8 medium (Thermo Fisher Scientific). We developed a novel fluorescent calcium indicator G-CaMP7.09. Briefly, a cDNA encoding G-CaMP7.09 was constructed by replacing the 1.13-kb SacI/ClaI fragment of G-CaMP7 cDNA with the corresponding 1.13-kb fragment of G-CaMP5.09 cDNA[25]. G-CaMP7.09 differs from G-CaMP7 by an N205S mutation in the circularly permutated, enhanced GFP (EGFP) domain and an L36M mutation in the calmodulin (CaM) domain (Extended Data Fig. 3a). The G-CaMP7.09 cDNA was subcloned into a pEGFP-N1 vector (Clontech) with a CMV promoter as described previously[25], for expression in cynomolgus iPSCs.

The G-CaMP7.09 plasmid was electroporated into cynomolgus iPSCs cultured in essential 8 medium supplemented with 10 mM Y-27632 (Thermo Fisher Scientific). The electroporation conditions were 1400 V pulse voltage, 10 ms pulse width and 2 pulses. Transfected cells were selected with 100 μg ml^{-1} G418 for 7 days. Successful transfection was confirmed by identification of green fluorescence by flow cytometry.

Karyotype analysis of cynomolgus iPSCs. The iPSCs were treated with 0.025 μg ml^{-1} colcemid for 4 h. The cells were collected by trypsinisation, incubated in 0.075 M KCl for 15 min, and fixed with methanol and acetic acid (3:1). Then, the chromosomes were spread on slides. The chromosome spreads were stained with quinacrine mustard and Hoechst33258 to enumerate chromosomes, following a standard protocol. Images were captured using an Axio ImagerZ2 fluorescence microscope (Carl Zeiss GmbH).

RT–PCR analysis of cynomolgus iPSCs and iPSC-CMs. Total RNA was isolated from cynomolgus iPSCs, iPSC-CMs or adult heart, using an RNeasy mini kit (Qiagen). cDNA was synthesized from 1 μg of total RNA with superscript III (Invitrogen) according to the manufacturer's instructions. The cDNA was PCR-amplified using the following primers:

OCT4, 5′-CAGATCAGCCACATTGCCCAG-3′ and 5′-CAAAAGCCC TGGCACAAACTCT-3′; *NANOG*, 5′-CCTATGCCTGTGATTTGTGGG-3′ and 5′-AGGTTGTTTGCCTTTGGGAC-3′; *SOX2*, 5′-GGTTACCTCTTCC TCCCACTCC-3′ and 5′-CCTCCCATTTCCCTCGTTTT-3′; *TNNT2*, 5′-AAGG AAGCTGAAGATGGCCC-3′ and 5′-GGGCCTGCTTCTGGATGTAA-3′;

GAPDH, 5′-AATCCCATCACCATCTTCCAGGAG-3′ and 5′-CACCCTGT TGCTGTAGCCAAATTC-3′.

The thermal cycling conditions were as follows: denaturation at 94 °C for 30 s, 30 cycles of 10 s at 98 °C; 30 s at 55 °C for *GAPDH*, 60 °C for *OCT4*, *NANOG*, and *SOX2*; and 30 s at 68 °C; final extension at 72 °C for 1 min.

Immunohistochemical analysis of cynomolgus iPSCs for pluripotency markers. Cells were fixed with 2% paraformaldehyde for 10 min and stained with antibodies against OCT4 (clone: c-10), NANOG (rabbit polyclonal) and SSEA4 (clone: MC-813-70), followed by goat anti-mouse–594 or goat anti-rabbit–488 (Thermo Fisher Scientific).

Teratoma formation assay. Undifferentiated iPSCs (10^7) in PBS were injected into the adductor longus muscle of male Fox Chase SCID mice (Charles River). When subcutaneous tumours were apparent at the site of transplantation (typically 6 weeks post-transplantation), the mice were euthanized and the tumours were excised and fixed with 4% paraformaldehyde.

Mixed lymphoid reaction. *In vitro* mixed lymphoid reaction was performed as described previously[26] with modifications. Prior to enrolment, a 7-ml blood sample was collected from each animal via venous puncture of the femoral vein. Peripheral blood mononuclear cells (PBMCs) were isolated using a vacutainer cell preparation tube (BD Biosciences) according to manufacturer's instructions. Recipient animal-derived PBMCs (10^6) were co-cultured for 5 days with the same number of donor-derived PBMCs pre-treated with 25 μg ml^{-1} mitomycin C. The cellular proliferation was monitored using a 5-bromo-2′-deoxy-uridine (BrdU) labelling and detection kit (Roche) according to the manufacturer's instructions. The control sample consisted of recipient animal-derived PBMCs without donor-derived cells. BrdU incorporation was expressed relative to the control.

iPSC-CM preparation. Undifferentiated cynomolgus iPSCs were differentiated into iPSC-CMs using the matrix sandwich method[12]. Briefly, undifferentiated iPSCs were plated on a Matrigel-coated culture dish (Corning) and cultured in essential 8 medium for a few days. When the cells reached 80–90% confluency, Matrigel was added to the medium, and the cells were treated with activin A (R&D) and subsequently, bone morphologic protein 4 (BMP4; R&D). On day 14 after differentiation, the cells were exposed to glucose-free medium for 3 days to enrich cardiomyocytes[13]. The cells were heat-shocked and cryopreserved. Cardiac purity was determined by immunostaining of cTnT (clone CT3), followed by anti-mouse IgG1 conjugated with phycoerythrin, using a FACSCanto II (BD Biosciences). G-CaMP7.09 fluorescence was measured using a FACSCanto II. Before transplantation, 4×10^8 cells were thawed and processed using a previously reported pro-survival cocktail[11]. Cell viability was determined by a trypan blue assay.

Animal surgeries. Based on the national regulations and guidelines, all experimental procedures were reviewed by the Committee for Animal Experiments and finally approved by the president of Shinshu University and Ina Research.

For major surgeries, the animals were anaesthetized by intra-muscular injection of ketamine and xylazine, intubated with a tracheal tube (4-mm diameter), and ventilated with 1.5% isoflurane. Buprenorphine was routinely administered subcutaneously to provide post-operative pain relief. Blood pressure, ECG and oxygen saturation were monitored during surgery. Phenylephrine was administered intravenously to maintain appropriate blood pressure. After median sternotomy, a 4-0 silk suture was passed through the myocardium at the mid-left anterior descending (LAD) coronary artery and threaded through a polyethylene tube (SP110, Natsume). A silicon tube was placed on top of the polyethylene tube and was tied off with a suture (Supplementary Video 4). Before induction of myocardial infarction, 1 mg kg^{-1} lidocaine and 1000 U heparin were administered intravenously. The same dose of heparin was subsequently administered every h until reperfusion. After 3 h of occlusion of the mid LAD, the heart was reperfused by removing the tubing. Immune suppression was achieved by daily

intra-muscular injection of methylprednisolone and tacrolimus (Astellas Pharma Inc.). Methylprednisolone was administered at 10 mg kg^{-1} day^{-1} from the day before transplantation for 3 days and at 1 mg kg^{-1} day^{-1} thereafter. Tacrolimus was administered at 0.1 mg kg^{-1} day^{-1}, 2 days before transplantation.

On day 14 after myocardial infarction, the animals underwent a second sternotomy and the heart was exposed. Either iPSC-CMs (4×10^8) suspended in PSC or PSC vehicle were delivered intra-myocardially into the infarct and border zones via 10 injections of 100 μl each using a 29-gauge injection needle.

Echocardiography. Echocardiography was performed on days −2, 28 and 84 relative to transplantation. After intra-muscular injection of the ketamine and xylazine anaesthetic mixture, the left-ventricular end-diastolic dimension (LVEDD), left-ventricular end-systolic dimension (LVESD) and heart rate were measured by transthoracic echocardiography (GE Vivid7) with a 10-MHz paediatric transducer. Fractional shortening (FS) was calculated using the following equation: FS = 100 × ((LVEDD−LVESD)/LVEDD). All measurements were taken over three consecutive cardiac cycles and averaged. An operator who was blinded to the study groups performed all measurements.

MicroCT. MicroCT was performed on the same days as echocardiography. Anaesthetized animals were intubated and mechanically ventilated with 1.5% isoflurane. Radiocontrast agent (Iopamiron Inj., Bayer) was infused at 8 ml min^{-1}. The hearts were imaged in an R_mCT AX (Rigaku, Japan), using the following settings: 80 kV; 500 μA; field of view, 100 mm. Motion cycles of cardiac contraction and ventilation were automatically synchronised by the μCT system. Left ventricular end-diastolic volume (LVEDV) and end-systolic volume (LVESV) were measured using Ziostation2 software (Amin). Left ventricular ejection fraction (LVEF) was calculated using this equation: LVEF (%) = 100 × ((LVEDV−LVESV)/LVEDV). An operator who was blinded to the study groups performed all measurements.

Holter ECG. The Holter ECG recordings were performed on days −2, 7, 14, 28, 42, 56, 70 and 80 relative to transplantation. The area intended for electrode placement was prepared by shaving. The electrodes were placed in a 2-lead precordial system and connected to a Holter recorder. A jacket was placed on the animal to protect the ECG system and a 24-h ECG was recorded. Ventricular tachycardia was defined as four or more consecutive premature ventricular complexes with a ventricular rate faster than 180 bpm. Sustained ventricular tachycardia was defined as ventricular tachycardia sustained longer than 30 s. An operator who was blinded to the study groups performed all analyses.

Blood test. Peripheral blood was collected on days 0, 28, 56 and 84 relative to transplantation. Plasma was isolated to measure BNP levels, using an automatic immunoenzyme assay kit (TOSOH). Whole blood was used to measure trough levels of tacrolimus by electrochemiluminescence immunoassay (SRL).

Fluorescence imaging of G-CaMP7.09-expressing iPS cell-derived cardiomyocytes. For *in vitro* fluorescent imaging, G-CaMP7.09-expressing cardiomyocytes were cultured on Matrigel-coated culture dishes (5×10^5 cells per cm^2) or stretchable parafilm (Bemis) for 7 days in 10% FBS (GIBCO)-containing IMDM (Sigma) with 1% MEM nonessential amino acid solution (Sigma) and 2 mM L-glutamine (Sigma). A fluorescence microscope (Olympus) was used to measure the fluorescence intensity of G-CaMP7.09. Ryanodine (50 μM), caffeine (5 mM, Wako), nifedipine (50 μM, Sigma) and BDM (20 mM, Wako) were added directly into the culture medium. Intravital imaging of the hearts grafted with G-CaMP7.09-expressing iPSC-CMs was performed on day 84 post-transplantation. After deep anaesthesia, iPSC-CM-transplanted hearts were injected with cold cardioplegia solution through the aorta (Miotecter; Mochida Pharmaceutical co.) and isolated. The hearts were transferred from the animal facility to the laboratory equipped with Langendorff setup. The hearts were reperfused at 37 °C with Tyrode's solution (containing 140 mmol l^{-1} NaCl, 1.8 mmol l^{-1} $CaCl_2$, 5.4 mmol l^{-1} KCl, 1 mmol l^{-1} $MgCl_2$, 11 mmol l^{-1} glucose, 5 mmol l^{-1} HEPES; bubbled with oxygen; pH 7.4). ECG (3 leads) and perfusion pressure was monitored continuously (PowerLab; ADInstruments). Epicardial G-CaMP7.09 signalling was optically recorded using a CCD camera (MiCAM02, Brainvision) through a band-pass filter (500–550 nm) when the heart was beating spontaneously or was paced at 3–4 Hz. To minimise motion artefacts, Tyrode's solution was supplemented with 15 mM BDM.

Histological analysis. On day 84 post-transplantation, the hearts were sectioned at 5-mm thickness and fixed with 4% paraformaldehyde. All sections were routinely stained with haematoxylin and eosin (HE) and picrosirius red to determine the scar region. Scar area was calculated by subtracting graft area from all fibrous areas (shown in red by picrosirius red staining) if the grafts were located in the scar (Extended Data Fig. 7i–k). The sections were immunohistologically analysed using primary antibodies against GFP (Novus, rabbit polyclonal), cTnT (clone: CT3), connexin 43 (Cx43, Abcam, rabbit polyclonal), CD45 (clone: 2B11&PD7/26/16), CD3 (clone: CD3-12), CD20 (clone: L26), CD31 (clone: JC/70A), pan cadherin (clone: CH-19), and sarcomeric α-actinin (clone: EA-53) followed by species-specific fluorescent (Molecular Probes) or biotin-conjugated (Vector Laboratories) secondary antibodies. For chromogenic detection, we used an HRP-conjugated streptavidin ABC kit (Vector Laboratories), followed by a DAB substrate kit (Vector Laboratories). Stained sections were imaged using a NanoZoomer 2.0-RS (Hamamatsu) or a Pulse-SIM BZ-X700 microscope (Keyence).

Statistical analysis. Ultrasound cardiography (UCG), μCT and BNP outcomes were analysed by an analysis of variance (ANOVA), followed by post-hoc comparisons between time points by Tukey's multiple comparison test, and unpaired *t*-test analysis to compare groups at each time point. For comparisons of the fraction of animals showing ventricular tachycardia, we used a two-sided Fisher's exact test. The percentage of cTnT and BrdU incorporation was analysed by ANOVA followed by post-hoc Tukey's multiple comparison tests. Correlations between ejection fraction and scar size or graft size were demonstrated by Pearson analysis. All statistical analyses were performed using GraphPad Prism, with the threshold for significance set at $P < 0.05$.

23. Robinson, J., Halliwell, J. A., McWilliam, H., Lopez, R. & Marsh, S. G. IPD--the immuno polymorphism database. *Nucleic Acids Res.* **41,** D1234–D1240 (2013).
24. Okita, K. *et al.* An efficient nonviral method to generate integration-free human-induced pluripotent stem cells from cord blood and peripheral blood cells. *Stem Cells* **31,** 458–466 (2013).
25. Ohkura, M. *et al.* Genetically encoded green fluorescent $Ca2^+$ indicators with improved detectability for neuronal $Ca2^+$ signals. *PLoS One* **7,** e51286 (2012).
26. Bigaud, M., Maurer, C., Vedrine, C., Puissant, B. & Blancher, A. A simple method to optimize peripheral blood mononuclear cell preparation from cynomolgus monkeys and improve mixed lymphocyte reactions. *J. Pharmacol. Toxicol. Methods* **50,** 153–159 (2004).

a

		DrpZ5-32B-C (iPS cell donor)		C035		C037		C038		C040		C043	
	Country	Philippines		Philippines		Philippines		Philippines		Philippines		Philippines	
	Sex	Male		Female		Female		Female		Female		Female	
Mafa Class I (MHC Class I)	Mafa-A	A1*089:03	A1*089:03	A1*089:03	A1*052:02	A1*089:03	A1*093:01	A1*089:03	A1*052:02	A1*089:03	A1*093:01	A1*089:03	A1*052:02
		A2*05:50	A2*05:50	A2*05:50	A4*01:04	A2*05:50	A1*074:02	A2*05:50	A4*01:04	A2*05:50	A1*074:02	A2*05:50	A4*01:04
		A3*13:03:01	A3*13:03:01	A3*13:03:01		A3*13:03:01	A8*01:01	A3*13:03:01		A3*13:03:01		A3*13:03:01	
	Mafa-B	B*104:03	B*104:03	B*104:03	B*095:01	B*104:03	B*095:01	B*104:03	B*095:01	B*104:03	B*041:01	B*104:03	B*095:01
		B*144:03N	B*144:03N	B*144:03N	B*033:02	B*144:03N	B*033:02	B*144:03N	B*033:02	B*144:03N	B*101:01:02	B*144:03N	B*033:02
		B*057:04	B*057:04	B*057:04	B*098:10	B*057:04	B*098:10	B*057:04	B*098:10	B*057:04	B*098:08	B*057:04	
		B*060:02	B*060:02	B*060:02		B*060:02		B*060:02		B*060:02		B*060:02	
		B*046:01:02	B*046:01:02	B*046:01:02		B*046:01:02		B*046:01:02		B*046:01:02		B*046:01:02	
		B*050:08	B*050:08	B*050:08		B*050:08		B*050:08		B*050:08		B*050:08	
		B*114:02	B*114:02	B*114:02		B*114:02		B*114:02		B*114:02		B*114:02	
		B*072:01	B*072:01	B*072:01		B*072:01		B*072:01		B*072:01		B*072:01	
	Mafa-I	I*01:12:01	I*01:12:01	I*01:12:01	I*01:11	I*01:12:01	I*01:11	I*01:12:01	I*01:11	I*01:12:01		I*01:12:01	I*01:11
Mafa Class II (MHC Class II)	Mafa-DRB	DRB1*03:21	DRB1*03:21	DRB1*03:21	DRB1*03:21	DRB1*03:21	DRB1*03:21	DRB1*03:21	DRB*W1:08	DRB1*03:21	DRB*W1:08	DRB1*03:21	DRB1*03:21
		DRB1*10:07	DRB1*10:07	DRB1*10:07	DRB1*10:07	DRB1*10:07	DRB1*10:07	DRB1*10:07	DRB*W36:01	DRB1*10:07	DRB*W36:01	DRB1*10:07	DRB1*10:07
									DRB*W3:01		DRB*W3:01		
	Mafa-DQA1	DQA1*01:07:01	DQA1*01:07:01	DQA1*01:07:01	DQA1*01:07:01	DQA1*01:07:01	DQA1*01:07:01	DQA1*01:07:01	DQA1*26:03	DQA1*01:07:01	DQA1*26:03	DQA1*01:07:01	DQA1*01:07:01
	Mafa-DQB1	DQB1*06:08	DQB1*06:08	DQB1*06:08	DQB1*06:08	DQB1*06:08	DQB1*06:08	DQB1*06:08	DQB1*18:07	DQB1*06:08	DQB1*18:07	DQB1*06:08	DQB1*06:08
	Mafa-DPA1	DPA1*02:05	DPA1*02:05	DPA1*02:05	DPA1*02:05	DPA1*02:05	DPA1*02:05	DPA1*02:05	DPA1*04:02	DPA1*02:05	DPA1*02:15:02	DPA1*02:05	DPA1*02:05
	Mafa-DPB1	DPB1*15:04	DPB1*15:04	DPB1*15:04	DPB1*15:04	DPB1*15:04	DPB1*15:04	DPB1*15:04	DPB1*03:04	DPB1*15:04	DPB1*10:01	DPB1*15:04	DPB1*15:04

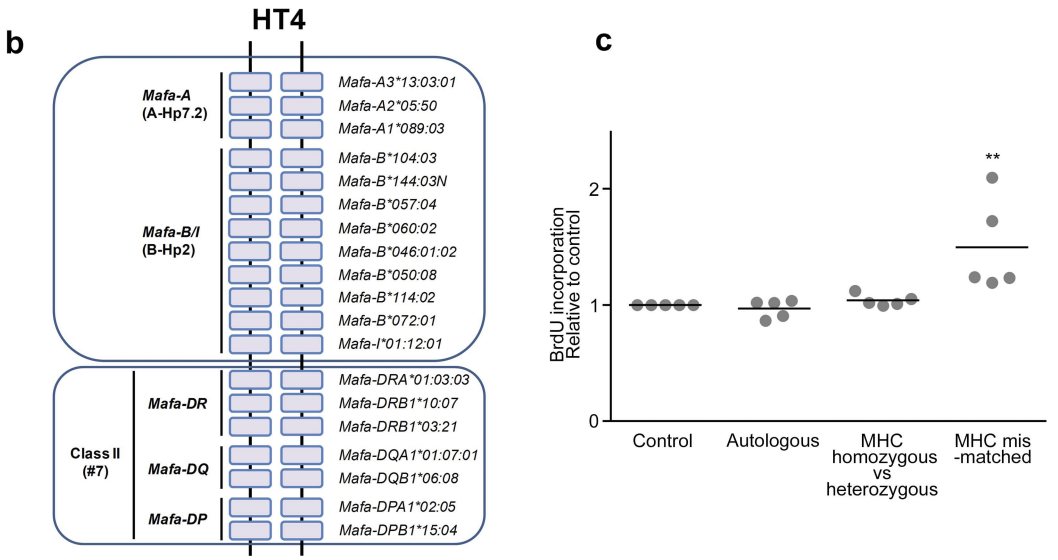

Extended Data Figure 1 | Characteristics of the HT4 haplotype. **a**, **b**, Basic structure of MHC in HT4 haplotypes. One of the cynomolgus monkeys (DrpZ5-32B-C) is strictly a 'homozygote' that has the A-Hp7.2 and B-Hp2 haplotypes in the Mafa-class I region and the #7 haplotype in the Mafa-class II region on both chromosomes (tentatively named 'HT4'). **c**, *In vitro* mixed lymphoid reactions (MLR) showed that when inactivated lymphocytes from a HT4-heterozygous monkey were cocultured with active lymphocytes from a HT4-homozygous monkey, proliferation was inhibited to the level of control (only inactivated cells) or autologous (inactivated and active cells from same animal). 'MHC mismatched' indicates two groups of lymphocytes from two different animals with different MHC types. $^{**}P < 0.01$ versus control. $n = 5$ per group.

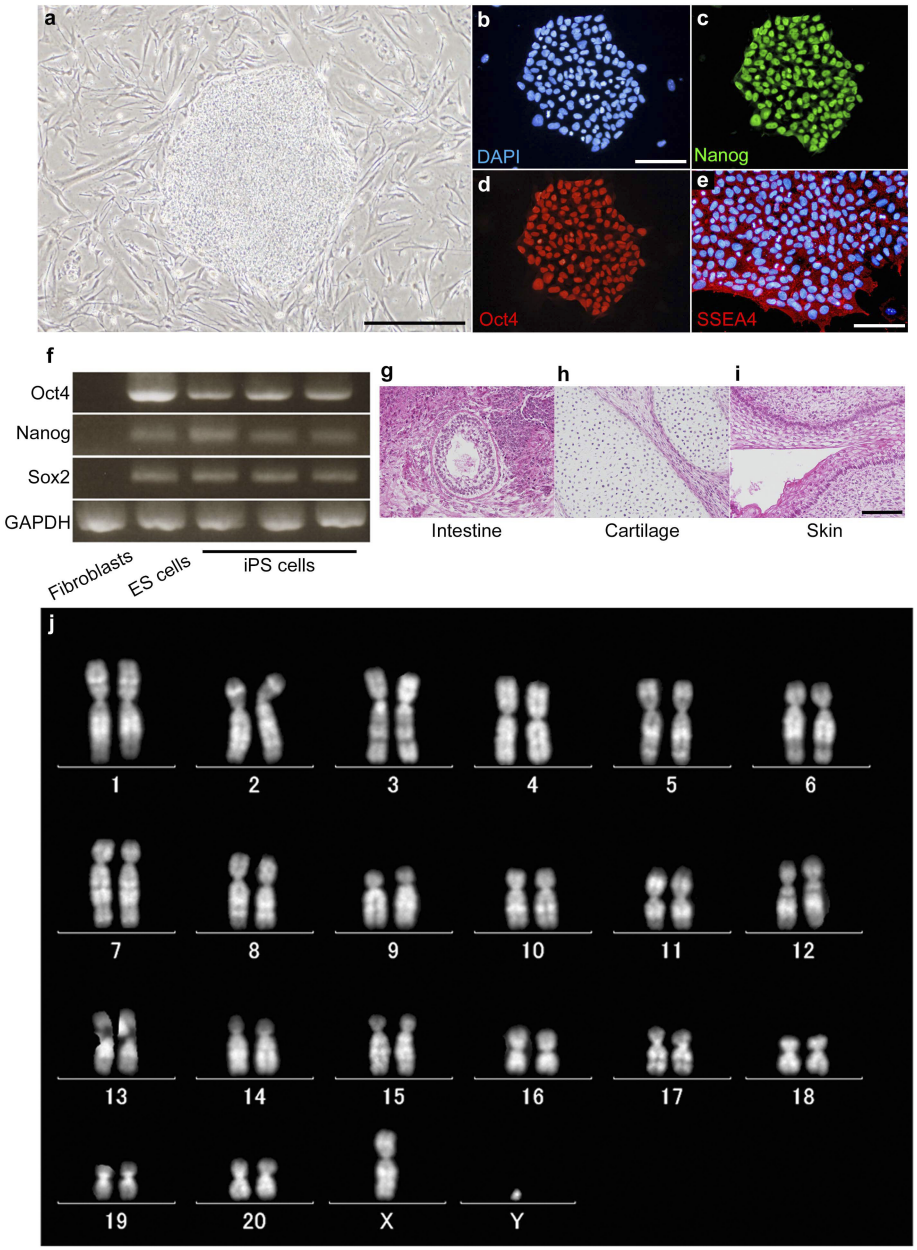

Extended Data Figure 2 | Generation of iPSCs from a MHC homologous cynomolgus monkey. Donor iPSCs were established from skin fibroblasts by transfection of episomal vectors carrying *OCT4, KLF4, SOX2* and *L-MYC*. **a**, iPSCs form typical ES-cell-like colonies. Scale bar, 50 μm. **b–e**, iPSCs express pluripotent markers as assessed by immunofluorescence. Scale bars, 100 μm. **f**, Gene expression of pluripotent markers in the iPSCs is identical to that in cynomolgus ES cells. **g–i**, When transplanted into immunodeficient mice, the iPSCs gave rise to teratomas manifesting all three germ layers: endoderm (intestinal epithelium), mesoderm (cartilage) and ectoderm (squamous cells). **j**, After expansion, the iPSCs showed normal karyotype (42, XY).

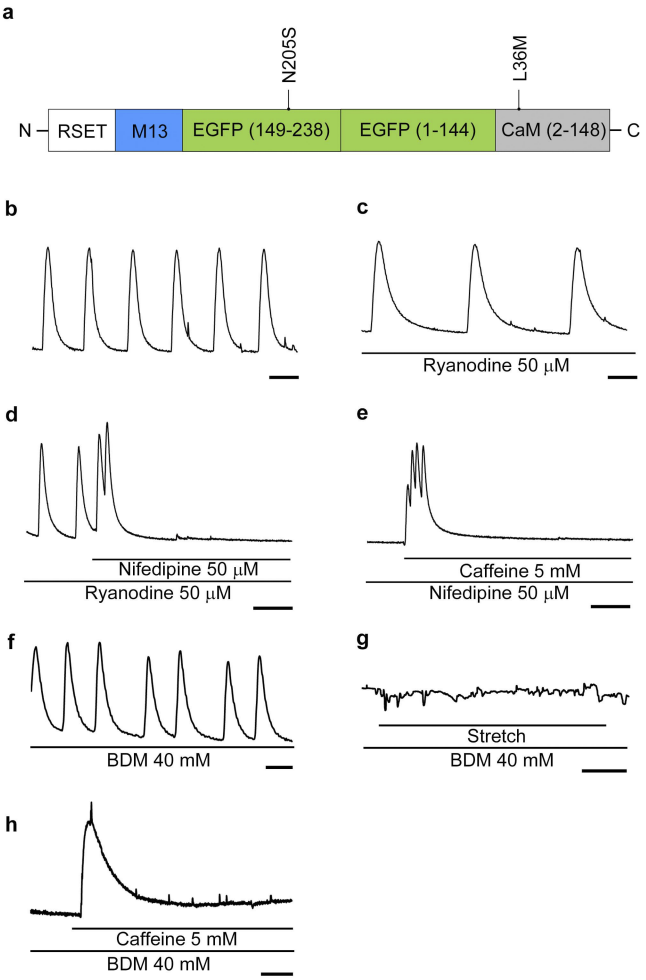

Extended Data Figure 3 | Characteristics of G-CaMP7.09. a, Schematic structure of G-CaMP7.09. Mutations are indicated with respect to G-CaMP7. RSET and M13 are tags that encode hexahistidine and a target peptide for Ca^{2+}-bound CaM derived from myosin light chain kinase, respectively. The amino-acid numbers of EGFP and CaM are indicated in parentheses. The dynamic range of G-CaMP7.09 (F_{max}/F_{min}) was 19.3 ± 2.52 ($n = 3$) and the K_d for Ca^{2+} was 212 ± 6.9 nM ($n = 3$). **b**–**h**, *In vitro* fluorescence transients of G-CaMP7.09-expressing cardiomyocytes. Data are representative of three independent experiments. **b**, Spontaneous contraction. Scale bar, 2 s. **c**, The firing rate of G-CaMP signals was reduced by treatment with ryanodine, a ryanodine receptor blocker. Scale bar, 2 s. **d**, Addition of the L-type calcium-channel blocker, nifedipine, resulted in cessation of fluorescent transients. Scale bar, 6 s. **e**, Treatment with an activator of the ryanodine receptor, caffeine, induced fluorescent transients in the G-CaMP7.09-expressing iPSC-CMs. Scale bar, 6s. **f**, G-CaMP7.09 transients were sustained for a few minutes after spontaneous contraction and stopped by 40 mM BDM. Scale bar, 1 s. **g**, After cessation of spontaneous fluorescent transients, iPSC-CMs on Parafilm were stretched but no fluorescent transient was detected. Scale bar, 10 s. **h**, Treatment with caffeine induced G-CaMP7.09 transients again. Scale bar, 5 s.

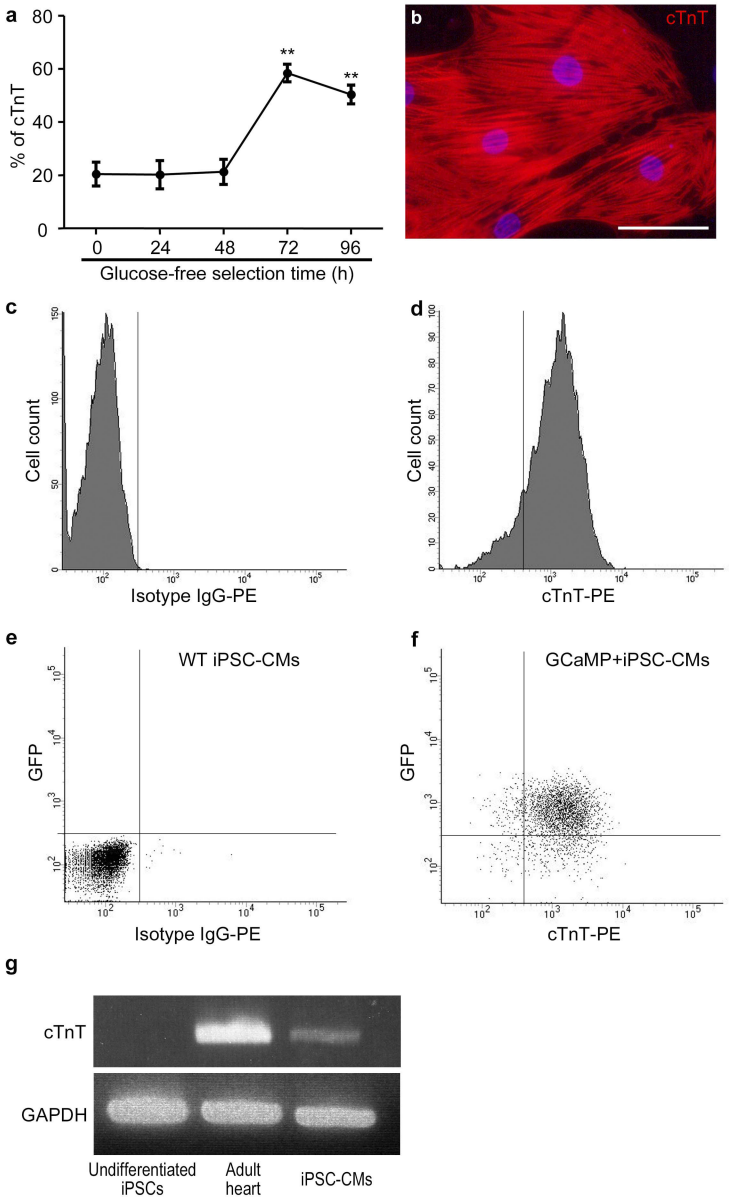

Extended Data Figure 4 | Generation and purification of cynomolgus iPS cell-derived cardiomyocytes. a, Pilot experiments showed that cultivation of iPSC-CMs in glucose-free medium for 72 h significantly enhances cardiac purity, $^{**}P < 0.01$ versus 0 h, $n = 4$ for each time point. Data are representative of three independent experiments. **b**, iPSC-CMs express the cardiac-specific marker cTnT. Scale bar, 50 μm. **c**, **d**, After multiple attempts to generate cardiomyocytes for transplantation, 2×10^9 cardiomyocytes (cTnT-positive $83.8 \pm 1.0\%$ as indicated by flow-cytometric analysis) were prepared. **e**, **f**, The cardiomyocytes were positive for GFP. **g**, RT–PCR analysis indicated that cTnT mRNA expression in iPSC-CMs was detectable, but lower than in the adult heart. Data are representative of three independent experiments.

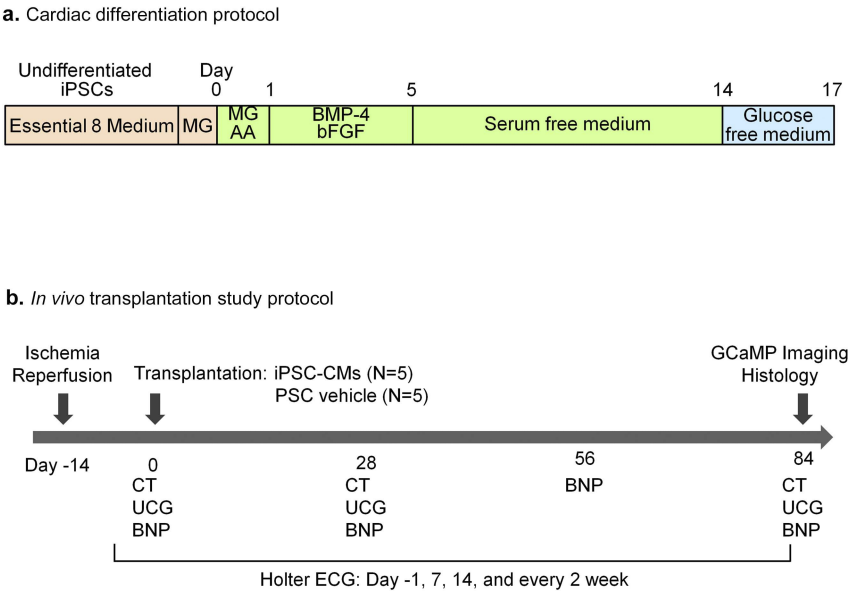

Extended Data Figure 5 | Study protocol and design. a, A monolayer of cultured undifferentiated cynomolgus monkey iPSCs on a Matrigel (MG)-coated dish was treated with Matrigel. The culture medium was replaced with serum-free medium supplemented with Matrigel and activin A (AA) on day 0. On day 1 after activation, the medium was replaced with medium containing BMP4 and basic fibroblast growth factor (bFGF), and cells were cultured until day 5. On day 14, cardiomyocytes were selected by cultivation in glucose-free medium for 3 days. **b**, Fourteen days before transplantation, 10 female monkeys were subjected to ischaemia/reperfusion injury. Either 4×10^8 iPSC-CMs reconstituted in a prosurvival cocktail (PSC) or the PSC vehicle was injected on day 0. Cardiac μCT and UCG were performed to evaluate cardiac contractile function before and after transplantation. Additionally, BNP was measured. Spontaneous arrhythmias were monitored by Holter electrocardiogram (ECG) on days −1, 7, 14 and every other week thereafter. On day 84, all animals were euthanized, and the hearts were excised and subjected to intravital G-CaMP imaging, followed by histological analysis.

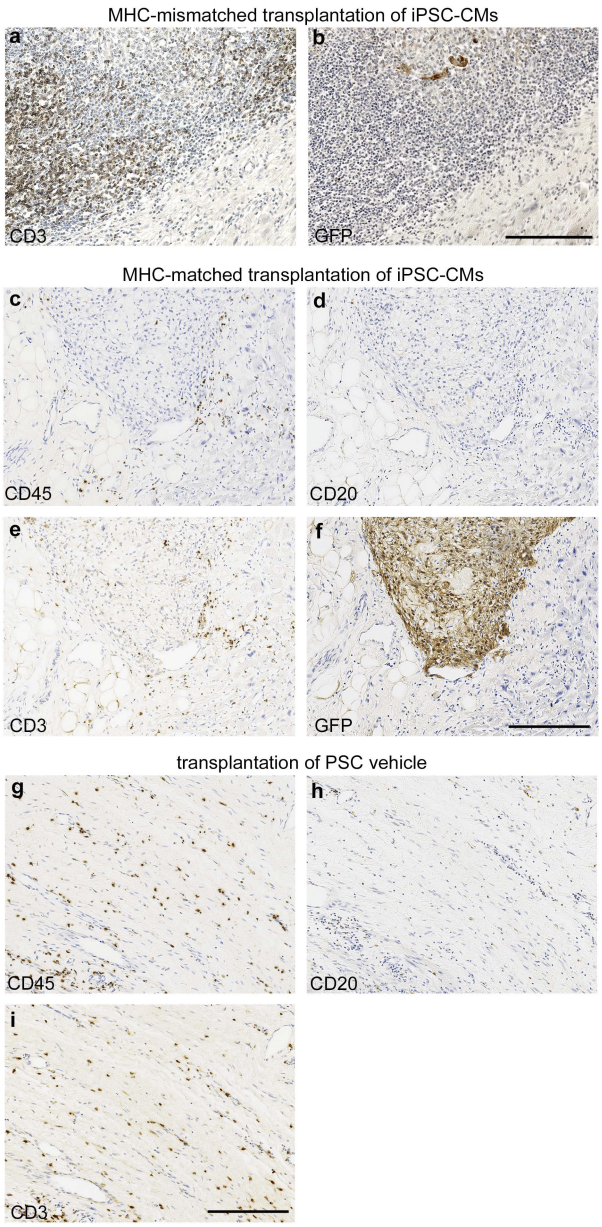

Extended Data Figure 6 | Immune response following transplantation of iPS cell-derived cardiomyocytes. a, **b**, iPSC-CMs were transplanted into MHC-mismatched infarcted hearts ($n = 2$). Animals were euthanized and the hearts were collected at 4 weeks post-transplantation. Only a small portion of grafts (GFP) showed a severe infiltration of inflammatory cells, such as $CD3^+$ T lymphocytes. **c**–**i**, Immunohistochemical analysis of recipients of iPSC-CMs or PSC vehicle 84 days post-transplantation. The sections were stained with antibodies against CD45 (leukocytes), CD20 (B lymphocytes), CD3 (T lymphocytes) and GFP (graft). Scale bars in **a**–**i**, 200 μm.

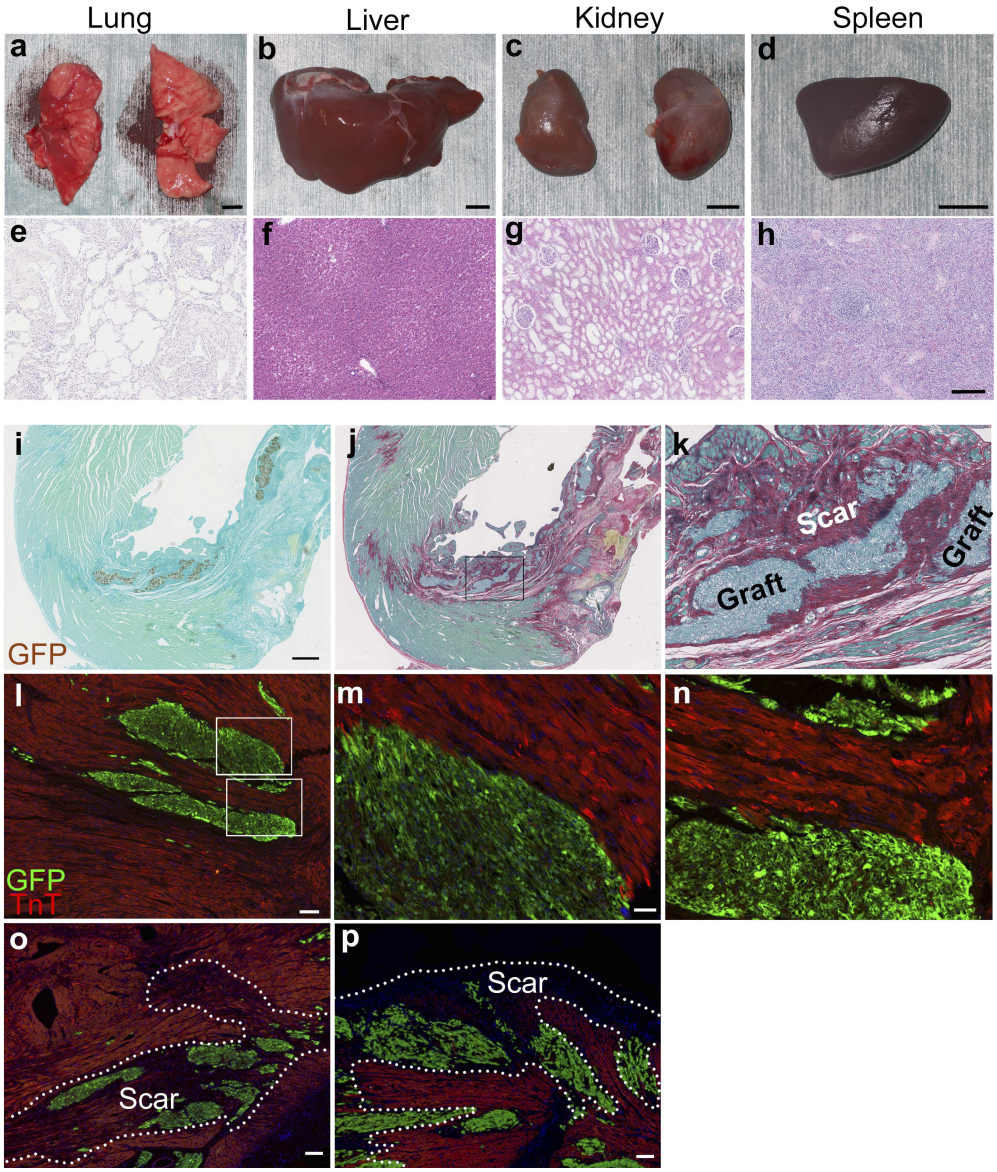

Extended Data Figure 7 | Macroscopic and microscopic analysis of iPSC-CM recipients. a–h, All recipients of iPSC-CMs received full necropsy after euthanasia. Neither macroscopic (**a–d**) nor microscopic (**e–h**) analysis revealed any evidence of tumour formation at 12 weeks post cell transplantation. Scale bars in **a–d** and **e–h**: 10 mm and 200 μm, respectively.**i–p**, Additional immunohistochemical analysis of cynomolgus hearts. **i**, Immunohistochemistry for GFP (brown) counterstained with fast green. Scale bar, 1 mm. **j**, **k**, Picrosirius red staining of a section in close proximity to the visual field in **a** shows partial remuscularisation of the scar (shown in red) by grafted cardiomyocytes. **l–n**, Different sections (lower by 5 mm towards the apex) showing the corresponding 2 grafts from Fig. 1b. Scale bar, 200 μm. **m**, **n**, Magnified images of the grafts, scale bar, 50 μm. Note the more direct contact zone of grafted cardiomyocytes with host myocardium. **o**, **p**, Additional examples of grafted cardiomyocytes in the scar and the border zone. Scale bars, 200 μm.

a

ID	Gender	Age (year)	BW (kg)	Treatment	%Graft area/Scar	%Graft area/LV	%Scar area/LV	EF on Day 84 (%)	# of grafts by histology (scar/total)	# of grafts by intravaital imaging (coupled/total)
C034	Female	5	3.2	PSC-vehicle	N/A	N/A	8.2	51.3	N/A	N/A
C035	Female	5	3.45	iPSC-CMs	8.1	0.83	10.3	55.2	3/4	2/2
C036	Female	5	2.83	PSC-vehicle	N/A	N/A	10.1	45.5	N/A	N/A
C037	Female	5	2.93	iPSC-CMs	12.4	1.19	9.6	62.1	4/6	3/3
C038	Female	5	2.6	iPSC-CMs	35.6	1.82	5.1	65.6	8/10	4/4
C039	Female	5	3.01	PSC-vehicle	N/A	N/A	12.2	40.7	N/A	N/A
C040	Female	4	3.14	iPSC-CMs	15.8	1.36	8.6	62.1	5/8	3/3
C041	Female	4	3.21	PSC-vehicle	N/A	N/A	11.4	54.4	N/A	N/A
C042	Female	4	2.88	PSC-vehicle	N/A	N/A	9.1	52.2	N/A	N/A
C043	Female	4	2.87	iPSC-CMs	9.6	1.02	10.6	55	3/4	2/2

b

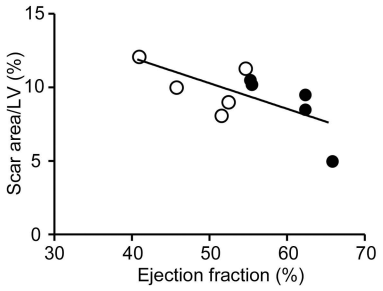

c

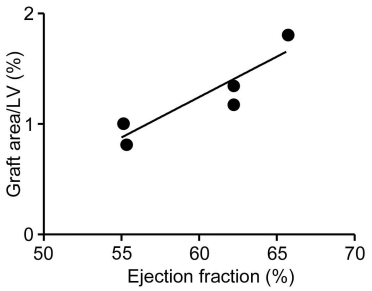

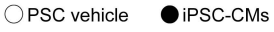

d

ID	day7			day14			day28			day42			day70		
	# of VTs	max duration (h:m:s)	max HR	# of VTs	max duration (h:m:s)	max HR	# of VTs	max duration (h:m:s)	max HR	# of VTs	max duration (h:m:s)	max HR	# of VTs	max duration (h:m:s)	max HR
C035	208	1:28:29	212	1	24:00:00	249	13	1:56	187	0	N/A	N/A	0	N/A	N/A
C037	149	3:29:54	223	1	24:00:00	249	74	12:52:00	216	91	0:22:25	211	34	0:22:15	216
C038	0	N/A	N/A	3	0:00:58	184	0	N/A	N/A	3	0:00:58	180	0	N/A	N/A
C040	0	N/A	N/A	3	0:00:59	184	83	0:53:45	225	2	0:0058	180	0	N/A	N/A
C043	0	N/A	N/A	48	1:24:52	202	0	N/A	N/A	0	N/A	N/A	0	N/A	N/A

Extended Data Figure 8 | Summary of histological, mechanical and electrophysiological consequences. a, Animal characteristics with histological, mechanical and calcium imaging results. **b**, Correlation between ejection fraction (EF) and scar area relative to left ventricular area (LV). **c**, Correlation between ejection fraction and graft area relative to left ventricle. **d**, Summary of sustained ventricular tachycardia (VT), including number of VTs, maximum duration, and maximum heart rate (HR), in the recipients of iPSC-CMs.

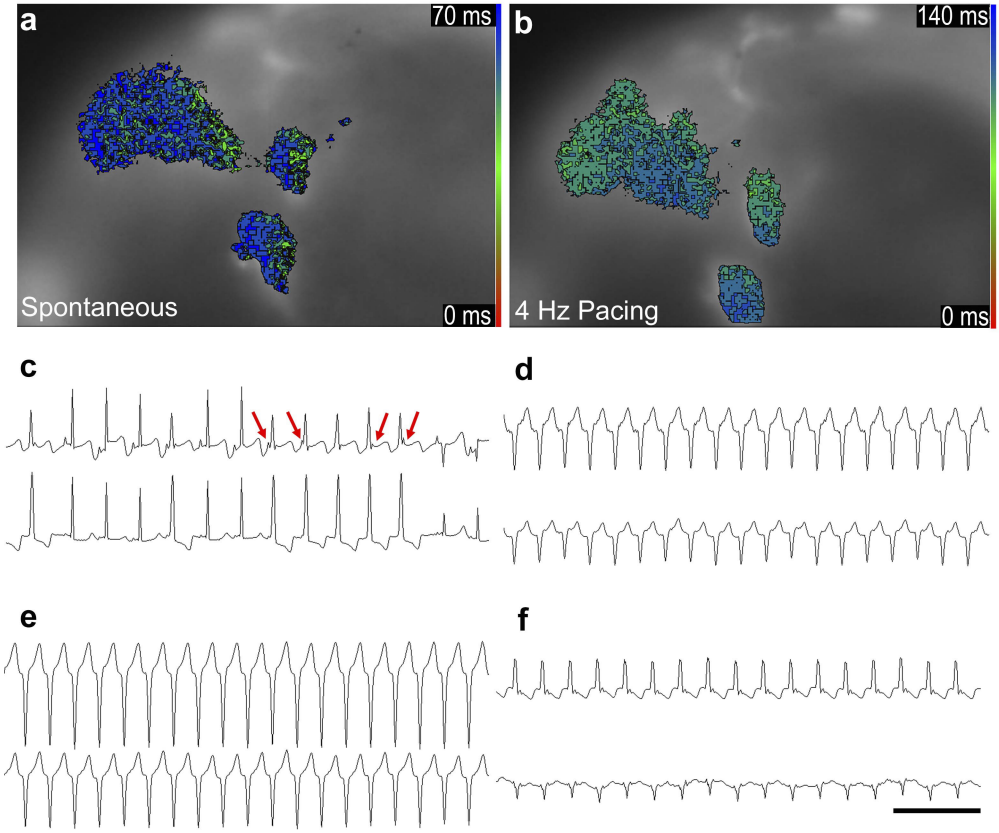

Extended Data Figure 9 | Additional electrical analysis of hearts transplanted with iPSC-CMs. a, **b**, Activation map obtained from G-CaMP7.09 transients showing the interval (in ms) between the R wave of ECG and the peak of the G-CaMP7.09 fluorescent signal. **c**–**f**, Examples of sustained and non-sustained VT in recipients of iPSC-CMs. Arrows indicate P wave during VT, suggesting atrioventricular dissociation. Scale bar, 1 s.

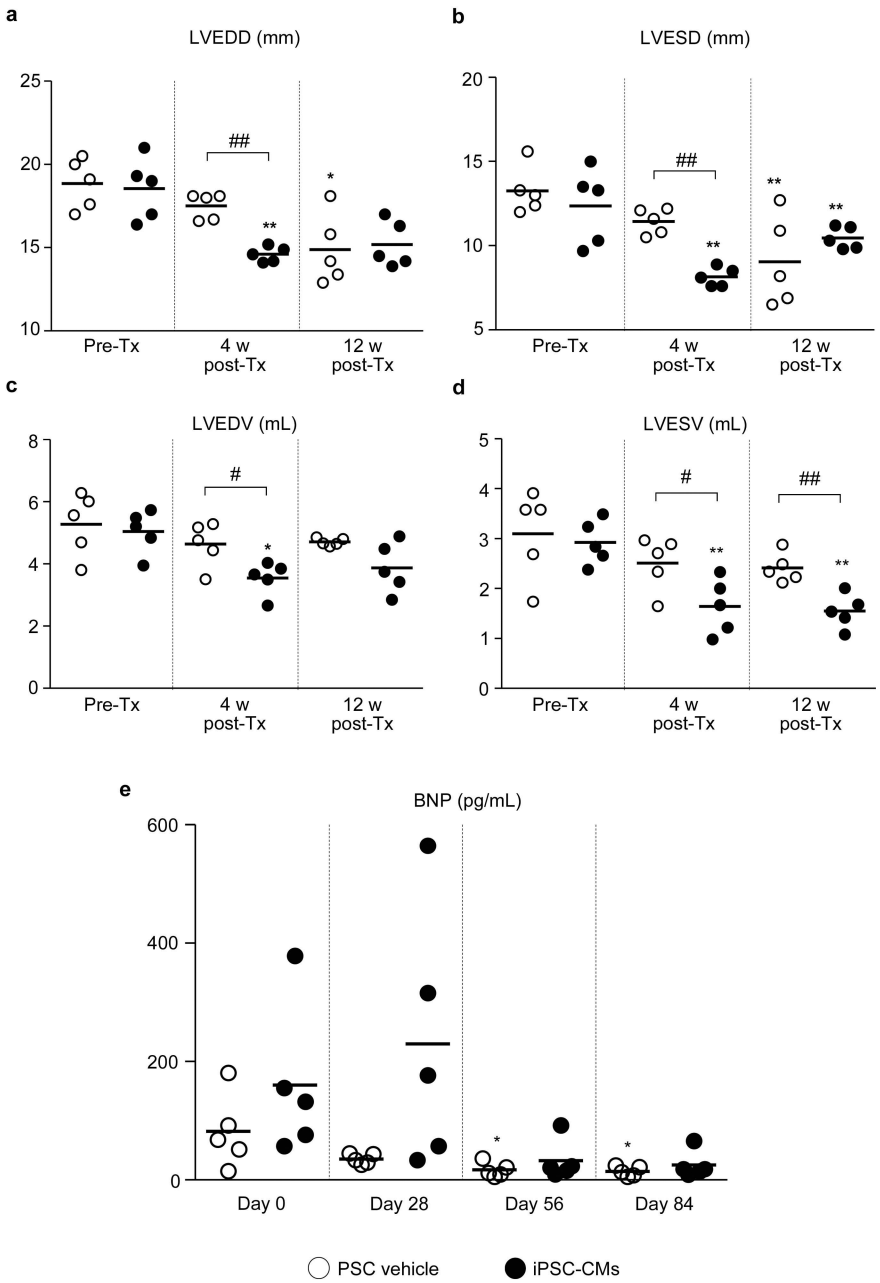

Extended Data Figure 10 | Time course of left ventricular size and BNP levels. a–d, Left ventricular size was analysed before transplantation (Pre-Tx), 4 weeks post-transplantation (4 w post-Tx) and 12 weeks post-transplantation (12 w post-Tx) by echocardiography (**a**, **b**) and μCT (**c**, **d**). LVEDD: left ventricular end-diastolic dimension, LVESD: left ventricular end-systolic dimension, LVEDV: left ventricular end-diastolic volume, LVESV: left ventricular end-systolic volume. $n = 5$ per group. $^{\#}P < 0.05$; $^{\#\#}P < 0.01$. * $P < 0.05$; ** $P < 0.01$ versus Pre-TX. **e**, BNP was measured on days 0 (14 days after myocardial infarction), 28, 56 and 84. No significant difference was detected between recipients of iPSC-CMs and recipients of PSC vehicle at any time point. * $P < 0.05$ versus day 0.